

Received 25 November 2024, accepted 7 December 2024, date of publication 17 December 2024,  
date of current version 30 December 2024.

Digital Object Identifier 10.1109/ACCESS.2024.3519488

## RESEARCH ARTICLE

# Transfemoral Prosthesis With Ambulatory Length-Actuation: Design and Preliminary Evaluation

THERESE E. PARR<sup>1</sup>, JOHN D. DESJARDINS<sup>1</sup>, ALAN R. HIPPENSTEAL<sup>2</sup>, TYLER G. HARVEY<sup>1</sup>,  
AND GE LV<sup>1,3</sup>, (Member, IEEE)

<sup>1</sup>Department of Bioengineering, Clemson University, Clemson, SC 29634, USA

<sup>2</sup>Prisma Health Department of Physical Medicine and Rehabilitation, Greenville, SC 29605, USA

<sup>3</sup>Department of Mechanical Engineering, Clemson University, Clemson, SC 29634, USA

Corresponding author: Ge Lv (glv@clemson.edu)

This work was supported in part by Clemson Creative Inquiry and in part by the Award 2340261 of the National Science Foundation.

This work involved human subjects or animals in its research. Approval of all ethical and experimental procedures and protocols was granted by Clemson University's Institutional Review Board Under Application Nos. IRB2021-0889 and IRB2022-0496.

**ABSTRACT** Most current powered transfemoral prostheses are designed based on replicating normal anatomy with the inclusion of a revolute knee joint. Prosthesis users often have issues achieving proper leg length to maintain balance and perform push-off during stance, and to ensure sufficient toe clearance during swing. There is a clinical opportunity to develop a powered prosthesis that linearly shortens and lengthens during ambulation with a prismatic joint for improved leg length properties. To build on previous work, the research in this manuscript focuses on designing the physical device, the leg length actuation profile, and the control scheme. Based on gait analyses of two prosthesis users, the device provides an appropriate leg length actuation profile with sufficient shortening for toe clearance (exhibited by the greater prosthetic vs. intact side toe clearance) and lengthening for forward propulsion (exhibited by the ground reaction force peak in late stance). The device also has a motor torque and velocity capable of supporting up to a 90 kg user during normal ambulation, a control scheme with an adjustable actuation cycle based on gait cadence (matching within 2 ms), and a more compact mechanical system design (4.5 kg) less than anatomical weight requirements (5.5 kg). Additionally, the prosthesis users tested were highly encouraging of their stability, mobility, and safety while ambulating with the device.

**INDEX TERMS** Prosthetics, biomechanics, biomechatronics, artificial limbs, assistive robots.

## I. INTRODUCTION

By the year 2050, it is expected that the population of persons with amputation will double to around 3.6 million [1]. Most individuals who undergo transfemoral amputations rely on a lower-limb prosthesis to perform activities of daily living. The functional goal for unilateral transfemoral prosthesis users during ambulation is to restore the proper biomechanics of gait and limit compensatory mechanisms that cause gait asymmetry [2], [3]. However, numerous clinical issues arise

The associate editor coordinating the review of this manuscript and approving it for publication was Jingang Jiang<sup>1</sup>.

because the majority of prevalent designs are based on replicating the structure of the missing limb while aiming to restore function.

Passive prostheses are composed of passive elements such as springs, dampers, and hinges [4]. These devices have the ability to lock the knee joint during stance to prevent buckling while in extension [5]. Swing control is dependent on constant mechanical stiffness, friction, and dampening; such devices are limited in functionality because they can only store and dissipate energy a user injects. The semi-active prostheses (e.g., the Ottobock C-leg [6]) are equipped with microprocessors to enhance stance

stability and augment swing control through regulating joint impedance via joint actuators. Recent advances of emerging powered prostheses [7], [8], [9], [10], [11], [12], [13] are able to generate net positive power for both action and reaction functionality. Active prostheses have an array of machine design features for enhancing stance stability, including lockable parallel springs, and ratchet or clutch locking mechanisms [14], [15], [16]. Swing distance and velocity is controlled with an actuator to produce a positive moment for both flexion and extension of the knee joint [14], [17]. Through refining actuation systems and control algorithms, these prostheses can restore normative kinematics for prosthesis users on different terrain conditions with minimal parameter tuning [11], improved comfort [8], [9], [10], and smooth transitions between tasks [7], [12].

While the above-mentioned prostheses have demonstrated promising results in assisting locomotion for prosthesis users, there exist many functional issues for lower mobility-level prosthesis users related to both stability and mobility. Prosthesis users continue to have an increased risk of falling and safety related concerns related to balance, stumbling, and knee buckling [18], [19] as well as gait compensations to achieve appropriate toe clearance on the prosthetic side during swing. In addition, without a powered ankle prosthesis, prosthesis users often experience plantar flexion deficiency on the prosthesis and insufficient forward propulsion during push-off [20]. The missing biomechanical function of the lower extremity leads to increased muscular effort of the residual and contralateral limbs [4], [20].

We hypothesize that a transfemoral prosthesis with a prismatic knee joint would eliminate knee buckling during stance and enable the user to directly control their leg length and the resulting biomechanical properties. Length-actuation of the prosthesis will focus on appropriate leg shortening for toe clearance and leg lengthening for push-off. The original concept of incorporating a prismatic joint in a kneeless linear prosthesis was introduced by Seliktar et al. [21], [22]. Biomechanical results from the prosthesis were improved stability, proprioception, and gait appearance, though the effective leg length profile was not ideal [22]. Our prior work proposed a refined design of length-actuated prosthesis (LAP) with fixed suspension and tethered setup, as well as an adjustable waveform [23]. The prosthesis was able to support the patient's full weight and adjust to the lengths needed during the gait cycle. Overall, the prototype and study proved that linear motion could replace the leg shortening functions of lower-joint rotations, with anecdotal improvements in kinematics and comfort.

In this paper, we focus on progressing our pilot prototype with novel effective leg length profiles based on anthropometric segment and joint characteristics. The length adjustment timing, including toe clearance and forward push-off, will be improved based on preliminary testing on non-disabled persons. In addition, this study will focus on integrating a more compact electromechanical drive system

(actuator and driver) for a self-contained prosthesis design and the elimination of the need to be tethered to the external motor and cam system. This paper also includes bench top testing of the LAP's weight tolerance, actuation profile, and control scheme, as well as preliminary testing on prosthesis users with walking experiments. Primary gait measurements include toe clearance and ground reaction forces because they are directly impacted by the actuation profile and performance of the LAP. Secondary measurements included sagittal plane kinematics and subjects' qualitative feedback on the overall performance and satisfaction.

The rest of the paper is organized as follows: in Sec. II we introduce various leg length profiles and the mechatronics design, in Sec. III we present bench top testing and results of the LAP and then in Sec. IV we present testing and results on two transfemoral prosthesis users ambulating with the device (Fig. 1). Finally, we discuss the meaning of the electromechanical and biomechanical results and possible future research directions in Sec. V.

## II. DEVELOPMENT OF THE PROSTHESIS

In this section, we propose the design of the leg length actuation profile and introduce the components of the LAP. We present the onboard sensors and the control structure to enforce the estimated leg length profile.

### A. LEG LENGTH ACTUATION PROFILE

The LAP's actuation profile has been extracted from our model to predict leg length throughout the gait cycle. This model measures dynamic leg length (DLL) according to the lengths of hip joint center to heel (HJC-HEEL,  $D_{\text{Heel}}$ ), hip joint center to ankle joint center (HJC-AJC,  $D_{\text{AJC}}$ ), and hip joint center to forefoot (HJC-FF,  $D_{\text{FF}}$ ) of normative gait. The lengths from HJC to HEEL, AJC, and FF were solved using trigonometry with the sides representative of thigh, shank, toe, and heel and angles representative of the normative ambulatory knee and ankle angles (Fig. 2). The expressions of these profiles are given as:

$$D_{\text{AJC}} = \sqrt{l_{\text{th}}^2 + l_{\text{sh}}^2 - 2l_{\text{th}}l_{\text{sh}} \cos \theta_k}, \quad (1)$$

$$D_{\text{FF}} = \sqrt{D_{\text{AJC}}^2 + l_{\text{t}}^2 - 2D_{\text{AJC}}l_{\text{t}} \cos(\eta + \theta_a)}, \quad (2)$$

$$D_{\text{Heel}} = \sqrt{D_{\text{AJC}}^2 + l_{\text{h}}^2 - 2D_{\text{AJC}}l_{\text{h}} \cos(\pi - \eta - \theta_a)}, \quad (3)$$

where  $\eta = \arccos((l_{\text{sh}} - l_{\text{th}} \cos \theta_k)/D_{\text{AJC}})$ ,  $\theta_k$  and  $\theta_a$  are the knee and ankle angles,  $l_{\text{th}}$ ,  $l_{\text{sh}}$ ,  $l_{\text{t}}$ , and  $l_{\text{h}}$  represent the lengths of a person's thigh, shank, toe, and heel, respectively. The original model to predict leg length was based on non-disabled anthropometric data [24], [25] but the sound limb of the prosthesis user can be measured to achieve a more accurate leg length profile.

During walking, the most distal part of the foot is critical in determining gait phases. Therefore, the most important measurement for proper leg length during terminal swing, heel strike, and loading response is HJC-HEEL, while

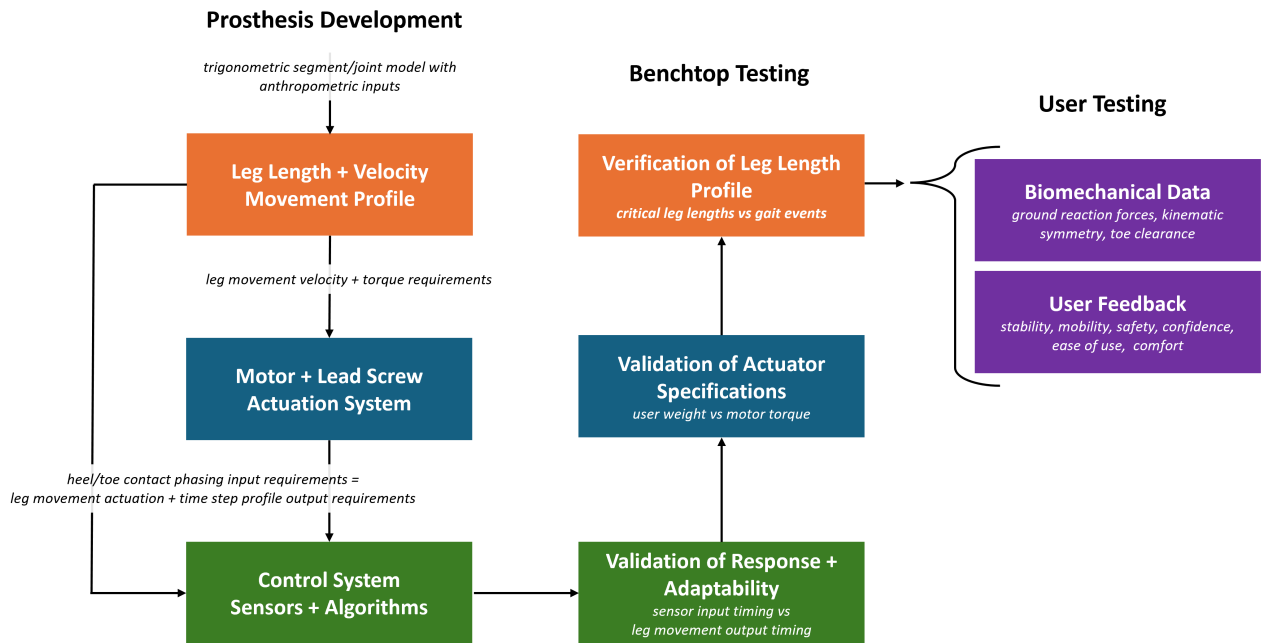


FIGURE 1. Research and development process of the length-actuated prosthesis detailed within this paper.

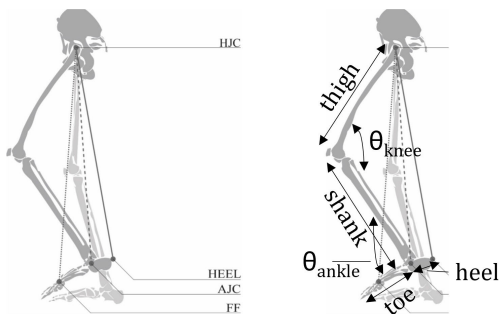


FIGURE 2. Anthropometric segments (thigh, shank, toe, heel) and dynamic joint angles (knee, angle) input into trigonometric predictive model.

terminal stance, push-off, and initial swing are dependent on HJC-FF. The prosthesis profile (HJC-AJC) was calculated with the critical length and hip joint angle during a gait cycle as inputs. The length profile was broken up into percentages of the gait cycle according to slope behavior; these slopes (position/percent of the gait cycle) were used to calculate the velocity of directional length changes. Position and velocity commands, as well as the ability to adjust timing to gait speed, were used in the control algorithm.

The DLL model profile of leg length assumes gait phases are determined by foot position, and bases HJC-AJC calculations on the progression of foot placement in normative gait. In addition to the DLL model profile, several other profiles were created to differ phase iterations. An Anatomical Hip (AH) model was developed to classify

gait phases by the orientation of the thigh/femur with the assumption that the prosthesis is an extension of this at all points in the gait cycle. These trajectory locations were solved for by using the thigh angle as the sole determinant for gait phase. Leg lengthening for push off and leg shortening for toe clearance will happen about 10% and 20% earlier, respectively, for the AH model compared to the DLL model based on foot location, because the thigh passes through late stance and mid-swing much earlier than the foot.

Another scenario we considered was the straight leg, or the locked knee (LK) model, which has been simulated before with a locked knee brace. This case shows that the hip flexion angle toe off and mid-swing are about 10% later than the healthy anatomical knee flexion angle model due to the inability of the heel to leave the ground on time with no knee bending [26].

The fourth actuation profile, the Combined model, uses the earliest push-off maximum from the AH model and the swing clearance minimum from the LK model. It has a slope similar to the DLL model between push-off and toe clearance, ensuring consistent and less demanding speed transitions. All profiles (DLL, AH, LK, and the combined) were tested and refined to develop a final actuation profile with accurate movement timings based on individual gaits (Fig. 3).

**B. PROSTHESIS ACTUATOR SYSTEM DESIGN**

The main requirements for the prosthesis actuator were to be able to achieve the speed and torque associated with the developed dynamic leg length profile. Additional device requirements included keeping the mass of the system below 5.5 kg, which is the mass for the below-knee anatomy [24],

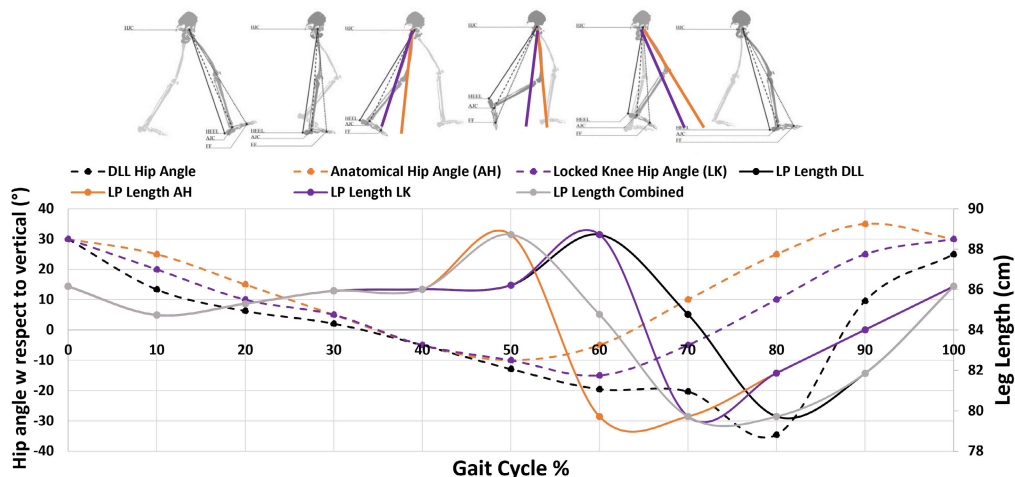


**FIGURE 3.** Illustration of leg length profiles (top) and calculated leg length profiles and hip angle throughout a gait cycle (bottom) for all proposed prosthesis length profiles (black - dynamic leg length, orange - anatomical hip angle, purple - locked knee, gray - combined).

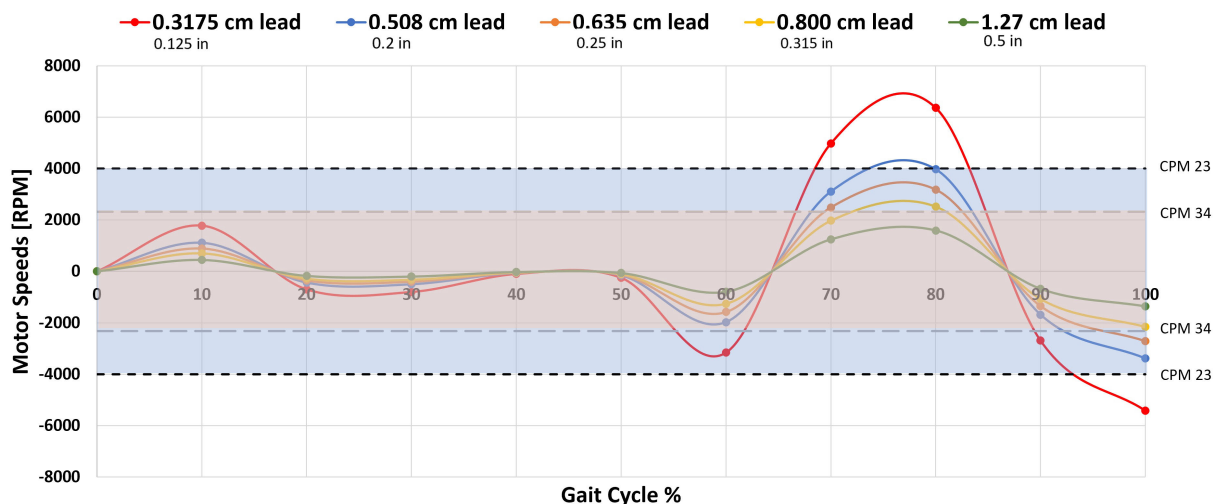


**FIGURE 4.** Motor speeds required by the full DLL profile for an array of lead screw distances and the NEMA ClearPath Motor (CPM) (blue).

[27], and towards the higher end of prosthetic legs in research (3.5 kg - 5.5 kg) [8], [10], [14], [28].

To configure parameters for the desired actuators, we divided the length change during every ten percent of a gait cycle by 0.15s (assuming a gait cycle of 1.5 m·s<sup>-1</sup>) to determine the velocity requirement of the actuator. We then conducted a weight analysis based on the selected lead screw to determine torque requirements of the actuator while considering mass of users and thread/friction angles. These have led us to a 120 W step and direction servo motor (NEMA 23, CPM-SDSK-2311S-RLN, ClearPath®, Teknic, Victor, NY), which can generate 2 Nm peak torque (0.4 Nm continuous torque) and reach a speed of 2320 revolutions per minute (RPM). This motor is able to achieve the actuation profile (maximum = 1974 RPM with 1.0 cm or 0.5 cm lead at 50% magnitude) (Fig. 4) and support the user’s weight,

meanwhile satisfying the range of power requirements similar to other transfemoral prostheses [15], [29], [30]. When calculating the maximum torque being exerted by the motor with a safety factor of at least 1.2, the motor should be able to hold up to 86 kg.

Once the motor had been determined, we fabricated a double pylon prototype with a motor mount using aluminum to serve as the basis for the prosthesis’ prismatic joint. The motor was located proximally on the lower limb and interface with a distally located ball screw to create telescopic motion (Fig. 5). The telescopic unit has the ability to connect to the distal pyramid of any standard prosthetic socket and to most standard prosthetic feet. We used the same Sidekicks™ prosthetic foot (CollegePark, Warren, MI) for the prosthesis as in our initial prototype [23] because it has a reduced toe length, which helps with newer prosthesis users’ adaptability

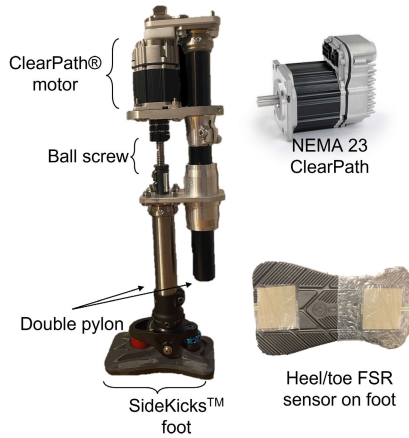


**FIGURE 5.** Overview of the prosthesis (left) with the selected NEMA 23 motor (top right) and the SideKicks™ prosthetic foot (bottom right).

and is often used as a training foot [31]. The reduced toe length and foot rigidity also simplifies the functional length waveform needed for toe clearance and preliminary evaluation of the LAP.

**C. SENSORS AND CONTROL STRUCTURE**

We adhered two force sensing resistors (FSRs) (FSR406, Interlink Electronics, Irvine, CA) to the bottom heel/toe of the prosthetic foot to detect stance vs. swing phases during walking. These FSRs were used as a quality measurement for presence of weight on the prosthetic leg rather than an exact measurement of force. The initial placement was flush to the edge of the front/back of the prosthetic foot for most accurate initial and final contact alerts. We first calibrated the FSRs based on the provided user manual to transform raw sensor readings into accurate force measurements, and then adjusted the threshold for detecting contacts through trials and errors. Requirements for the FSR included being able to identify foot strike and toe off within a threshold of around 20 N [32], [33], [34], which was standard for the chosen FSR according to the manufacturer’s specifications (0.2 N - 20 N sensitivity). Communication for the motor control loop and receiving sensory feedback was established through a motor driver (ClearCore, Teknic, Victor, NY). All the onboard electronics were powered by a compact power unit (Intelligent Power Center 5, ClearPath®, Teknic, Victor, NY), and a push button was included to control power to the actuator and allowance of leg length changes.

We divided the LAP gait control phases using the binary ON/OFF logic of the heel and toe FSRs based on the sensor readings exceeding above (rising edge) or decreasing below a pre-defined threshold (20 N). The LAP control phases included: 1) stance (heel ON, toe ON), 2) late stance (heel OFF), and 3) swing (toe OFF) as shown in Table 1. The beginning of stance, and the gait cycle, was defined as the moment the prosthetic heel makes contact with the ground and the heel FSR is characterized as ON. During

**TABLE 1.** Triggering logic of toe and heel FSR sensors and the corresponding phases.

Phase No.	Logic	Phase	Action
1	Heel FSR ON	Stance	Weight acceptance
1	Toe FSR ON	Stance Continued	Weight acceptance
2	Heel FSR OFF	Late Stance	Push-off
3	Toe FSR OFF	Swing	Toe clearance

stance, the prosthesis shortens for weight acceptance and then reaches neutral length. Between stance and late stance, the toe sensor should turn ON to ensure proper progression through the gait cycle; this was programmed as a requirement to move on to late stance but will not interrupt or change any movement. Late stance was activated by the heel FSR switching OFF while the toe is still ON; the LAP responds by lengthening for push-off. Swing phase was activated once the toe FSR decreased in force reading, and the prosthesis rapidly shortened for toe clearance and then returned to neutral length in preparation for the next heel strike.

**TABLE 2.** Maximum and average difference (in both time and percentage) between input pulse period and output prosthesis gait cycle timing in three varying speeds and period scenarios, as shown in Fig. 6.

Test	Max (ms)	Average (ms)	Max (%)	Average (%)
1	4	1.98	0.26	0.14
2	4	2.04	0.33	0.13
3	7	2.17	0.40	0.14

First, we set an initial gait cycle timing for the subsequent gait cycle to initiate leg movement without commanding the leg to move. Subsequent time between the initial and the end of a phase was calculated to determine a user’s gait periods and the velocity of the prosthesis. The gait cycle period and phasing distribution has the ability to increase and decrease, adjusting the speed of progression through the model to match the gait cycle timing and phasing of the user. If a user’s walking speed increases to trigger an early heel contact (as opposed to the pre-defined one), the prosthesis progresses to 10% of the DLL profile. Because the prosthetic foot is pliable, there is a tendency for the FSRs to misidentify heel contact versus toe off events. The control architecture accounts for this by rejecting strikes measured with a period less than 75% of the current cycle. If encountered, the motion continues and the period of the next cycle is set to the one previous of the false interrupt. On the other hand, the control algorithm accounts for missed identification of a new gait cycle by omitting cycles that are more than 125% of the pre-defined gait cycles. The desired motor position ( $D_m$ ; pulses) and velocity ( $V_m$ ; pulses/second) for each phase of the profile are given as

$$D_m = \frac{\Delta_L \cdot r}{l}, \quad V_m = \frac{\dot{\Delta}_L \cdot r}{l}, \quad (4)$$

where  $\Delta_L$  is the change in length (cm) of the leg over the relevant phase,  $l$  is the lead distance (cm/revolution) of the

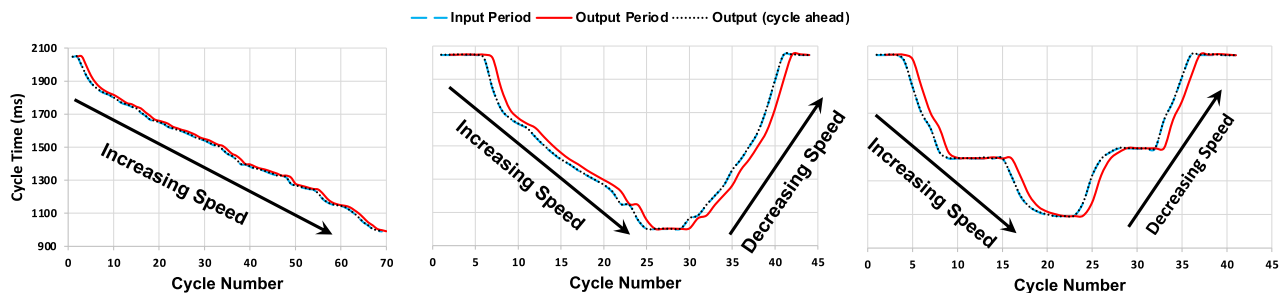


**FIGURE 6.** Input pulse period (blue) compared with the current (red) and next (black) output period by the LAP in varying speeds and period scenarios.

lead screw, and  $r$  is the resolution (pulse/revolution) of the motor (software-set constant = 800 pulse/revolution).

**III. BENCH TOP TESTING OF THE PROSTHESIS**

After prototyping, we conducted bench top testing to verify the performance of the prototype, including control adaptability, actuation system response, and the proposed leg length profiles.

**A. CONTROL ADAPTABILITY TESTING**

We tested the systems’ reaction time to triggers by connecting the actuator’s driver to an Arduino board that sends out impulse signals, which simulate strike activations. The input period between pulses was compared against the resulting time it takes for the prosthesis to run through the paired gait cycle. Increasing and decreasing walking speeds were simulated with adjustments to a potentiometer and the resulting time between sequential pulses so that the adjustments of the output period with respect to the input could be verified (Fig. 6 and Table 2). The average difference between the input and the output period was around 2 ms (0.14% in percentage), and the output timing was able to match the input within one gait cycle in every test. Additionally, we tested the device’s reactions to spurious triggering, *e.g.*, simultaneous triggering, missed triggering, and out of physiological order triggering of the FSRs via impulse signals to ensure the prosthesis will not initiate movement based on false events during a gait cycle.

**B. ACTUATION SYSTEM TESTING**

The ability of the prosthesis to safely withstand the weight of users was determined by measuring the Root-Mean-Square (RMS) of the maximum torque experienced by the actuator during ambulation. The motor torque is directly related to the amount of weight acting against it, and as it reaches its full capacity, the performance degrades until it powers off. To test this capacity, four non-disabled subjects (masses 62.2 kg, 93.1 kg, 96.3 kg, and 111.2 kg) walked on the treadmill while wearing the prosthesis and tracking the measured actuator torque. The maximum stable RMS torque of the motor was recorded for each participant (Fig. 7). The maximum torque, and subsequent motor shutdown, was reached while the

participant with a mass of 111.2 kg was ambulating. The torque results indicated that persons with a weight up to 90 kg may safely ambulate on the prosthesis with a factor of safety around 1.2. Additionally, the positional error while the system was counteracted by body weight during ambulation was only  $\pm 10$  counts, which comes out to a negligible distance of 1/80 of a revolution.

The mass of the linear component of the prosthesis was around 2.5 kg and the overall mass of the system with the addition of a bypass socket and foot was 4.5 kg. This is less than the typical human limb [24], [27], and also within the mass range of prevalent prostheses developed in the last ten years [8], [10], [14], [28].

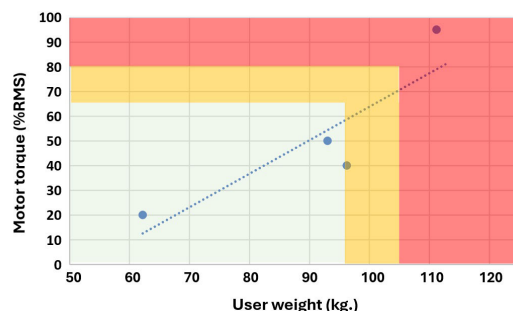


**FIGURE 7.** Four non-disabled subjects (blue dots) with increasing body weights walked on the prosthesis with full motion until it reached full RMS torque. Torque safety levels were classified as safe up to 65% (green), cautionary between 65% and 85% (yellow), and dangerous above 85% (red).

**C. LEG LENGTH PROFILE TESTING**

We consolidated the developed DLL profiles via walking experiments on a non-disabled subject. Gait phases and timings associated with the DLL profiles were refined based on the hip flexion as well as the qualitative feedback from the participant. Although we had only one non-disabled person for testing, this number has been considered acceptable in configuring prosthetic devices to ensure safety and to prove feasibility [35], [36], [37], [38]. Following approval from Clemson University’s Institutional Review Board (IRB2021-0889), one non-disabled participant (Female, 1.91 m, 65.5 kg) was recruited to participate in the walking experiments

while wearing the LAP. We installed a non-disabled bypass adaptor (Fig. 8) to act as a socket so that the participant can don the prosthesis with a 90° bent knee.

The testing consisted of five iterations of 3-minute walking trials on a split-belt force platform instrumented treadmill (Bertec, Columbus, OH) at  $0.67 \text{ m} \cdot \text{s}^{-1}$  with a 5-minute break in between each. For each trial, data was collected during the third minute of ambulation once the participant has acclimated to the prosthesis. The subject first walked on the treadmill without the prosthesis to have normative kinematics recorded and set as a control metric. The subject then walked with the prosthesis, which was randomly set to one of the four length profiles in which the subject was blinded to. A custom lower-limb model of the participant and the novel prosthesis was developed in Vicon motion capture system and Visual3D (C-Motion, Germantown, MD) to track and analyze the participant's motion.

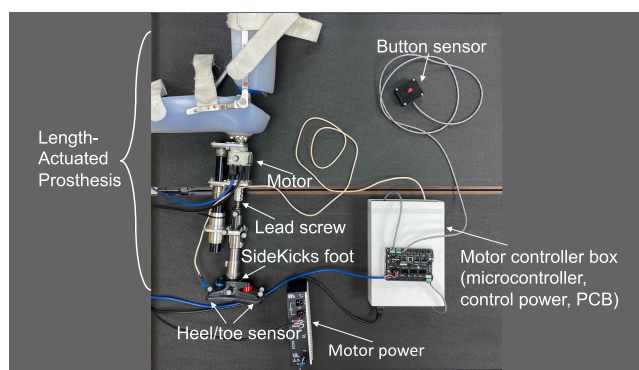


**FIGURE 8.** The developed LAP with a non-disabled bypass adaptor attached.

We computed the leg length as the difference between the virtual hip joint center marker and ankle joint center marker. Hip flexion was determined as the angle of the thigh segment about the x-axis in the sagittal plane. Heel strikes and toe offs were automatically identified by Vicon based on the ground reaction forces (GRFs) and imported into Visual3D to normalize the gait cycles (0-100%) and compare the hip flexion with dynamic leg length profiles. Results in Table 3 show that the proposed Combined model profile was able to achieve a shortening swing length within 1% during toe clearance and a maximum push-off length within 3% during terminal stance. All other leg length profiles fell outside these two ranges, and the subject's feedback confirmed unsatisfactory stability, balance, and timing of the mistimed models; most critically with the late models (DLL, LK) shortening during heel strike.

#### IV. EXPERIMENTS ON PERSONS WITH AMPUTATION

In this section, we demonstrate experimental results with two persons with transfemoral amputation wearing the developed LAP and their own habitual knees (HK) during treadmill walking.

#### A. HUMAN SUBJECTS AND EXPERIMENTAL DESIGN

Following approval from Clemson University's Institutional Review Board (IRB2022-0496), two individuals (demographics in Table 4) with transfemoral amputation were consented and recruited from local orthotic/prosthetic clinics and hospital systems to participate in this study.

Both subjects visited the laboratory a maximum of three times to complete the study. At the first visit, we measured the subject's anthropometry and vertical length from the distal end of their residual limb to the ground to prepare a prosthesis build height. Both subjects also provided their previous definitive sockets to the study team to prepare the assembly of the socket and prosthesis before the subsequent data collection visit. During the second visit, both subjects ambulated on the treadmill while wearing the LAP for multiple 30-second trials. The study team then fine-tuned the timing and magnitude of the length profile based on the feedback from both subjects to ensure maximum user comfort and control. During each walking trial, biomechanical data was collected to ensure that the best fit model was selected. The fine-tuning by the study team included moving the toe FSR further back along the foot to predict toe-off instead of reacting to toe-off and finalizing running a 1.0 cm lead profile on a 0.5 cm lead (50% magnitude). Both subjects came in two weeks later for a final visit to have data collected while wearing their own prostheses and the developed LAP. At the end of the final visit, both subjects answered a ranking and open-ended questionnaire to provide feedback on the LAP in comparison to their habitual device.

#### B. EXPERIMENTAL SET-UP AND DATA COLLECTION

For trials with the habitual prostheses and the intact side of subjects with the developed LAP, we placed reflective markers for the Vicon motion capture system following the standard Plug-in Gait model [39]. One additional marker was added to the first metatarsal for calculations involving the forefoot (*i.e.*, toe clearance distance and leg length). For trials with the LAP, the prosthetic side was marked with the same anatomical placements for the anterior-superior iliac crest, posterior superior iliac spine, and thigh, with two additional markers on the thigh segment (distal socket and motor), three markers on the shank, below the lead screw (one at the ball screw housing and the others at adaptor plate), and three markers on the prosthetic foot (two at toe and one at heel) (Fig. 9). A unique lower limb model of the subject and the LAP was developed in Vicon and Visual3D to track and analyze the motion of the subjects.

During the biomechanical data collection visits, subjects walked with their habitual prostheses for an accommodation period of five minutes to reach a desired speed of  $0.6 \text{ m} \cdot \text{s}^{-1}$  [40] and then had their kinematics recorded during steady-state walking. The subjects were then given a ten-minute break to change into the LAP and re-started walking until reaching a speed of  $0.6 \text{ m} \cdot \text{s}^{-1}$  to have their motion captured. After walking with both devices, both subjects gave

**TABLE 3.** Gait cycle percentage (%) that critical leg lengths (maximum and minimum) and gait events (terminal stance and mid-swing) occurred in comparison to one another. Maximum leg length should occur at the same percentage as terminal stance for push-off and minimum leg length should occur at the same percentage as mid-swing for toe clearance.

	Push-Off Timing (%)		Toe Clearance Timing (%)	
	Maximum Leg Length	Terminal Stance	Minimum Leg Length	Mid-Swing
AH Model	52	58	67	70
DLL Model	77	51	6	65
LK Model	82	52	8	64
Combined Model	57	60	72	73

open-ended feedback and ranked their devices and the LAP on stability, mobility, safety, confidence, ease of use, and comfort.



**FIGURE 9.** Subject 1 wearing his HK (left) and the developed LAP (right) attached with reflective markers.

**TABLE 4.** Subject demographics and their HKs.

Information	Subject 1	Subject 2
Age (yrs)	64	55
Gender	Male	Female
Height (m)	1.78	1.6
Weight (kg)	74.1	56.7
Amputation (yrs)	47	2
Amputation Cause	Trauma	Trauma
Amputation Side	Left	Right
MFCL	K3	K2
Prosthetic Knee	C-Leg (OttoBock)	Össur Total Knee
Prosthetic Foot	Össur Flex-Foot	Taleo (OttoBock)
Socket Type	Ischial Containment	Ischial Containment

**C. DATA PROCESSING**

All biomechanical data, including force plate measurements, and 3D marker trajectories were imported into Visual3D for analysis. Minimum toe clearance was solved within a custom Visual3D pipeline. The force plate measures automatically identified heel strike and toe off events based on rising GRFs, where the former event was used as the starting point of a gait cycle. Minimum toe clearance was calculated by determining the local maximum perpendicular distance (z-axis) of the first metatarsal marker between toe off and heel strike [41], [42]. The sagittal joint angles were calculated by the software for the hip, knee, and ankle by using the references of pelvis

and thigh, thigh and shank, and shank and foot, respectively. The frontal (y-axis) joint angles were calculated similarly to the sagittal; hip abduction and pelvic obliquity referenced the thigh to the pelvis, and the pelvis to the lab, respectively.

All joint angles and kinetic measurement from the force plates were filtered using a 4th-order low-pass Butterworth filter with 6 Hz and 35 Hz cutoff frequency, respectively [43], [44]. GRFs were normalized to the body weight of the subject [45]. With data sets for multiple steps, all discrete variables were compared between sides and between devices with an ANOVA and post-hoc Tukey’s test of the means with significance 0.05 in SPSS (IBM SPSS V28, IBM Corp., Armonk, NY, USA).

**D. BIOMECHANICAL RESULTS**

GRFs varied significantly between the two subjects (Fig. 10; Table 5). Subject 1 (S1) had significant differences for both initial loading (IL) and push-off (PO) peak GRFs between sides and devices for almost all conditions. S1 had higher loading on the intact side for both IL and PO with the habitual knee, but higher loading on the prosthetic side for both IL and PO for the LAP. Subject 2 (S2) had fairly similar loading between sides using the LAP, where PO peak was significantly less on the prosthetic side with her habitual device. Both subjects had larger impulses on their intact side, regardless of speed or device.

Kinematic gait symmetry is not possible to assess at the ankle or knee joint due to the locked and telescoping nature of the LAP. However, sagittal kinematics for the intact side ankle and knee, and bilateral hips were physiologically normal and similar between devices (Fig. 11). Notable differences between devices for both subjects was a higher intact side ankle flexion using the LAP and an earlier pre-swing hip flexion using the habitual device.

Overall toe clearance was consistently higher with the prosthetic side than with the intact side for all subjects, speeds, and devices (Table 5). S1 had higher toe clearance with the habitual knee prosthesis, and S2 had higher toe clearance with the developed LAP.

**E. QUALITATIVE RESULTS**

Both subjects were encouraging of the overall concept and believed that the device provided both stability and mobility, but were split when it came to comfort, ease of use, and confidence (Table 6). S1 was a microprocessor knee user

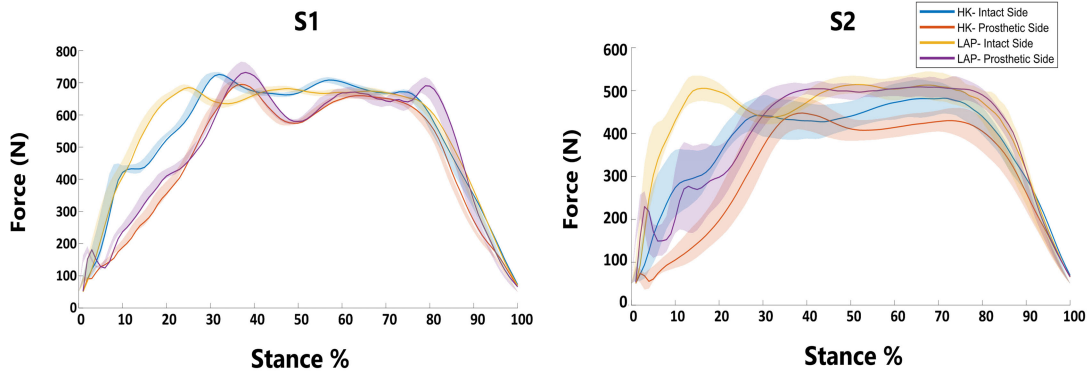


**FIGURE 10.** Mean  $\pm 1$  standard deviation of both subjects' bilateral GRFs while ambulating at  $0.6 \text{ m} \cdot \text{s}^{-1}$  with both their HK and the developed LAP.

**TABLE 5.** GRF and toe clearance comparison between devices.

		HK		LAP	
		Intact	Prosthetic	Intact	Prosthetic
S1, $0.6 \text{ m} \cdot \text{s}^{-1}$	IL Peak GRF (N)	$728 \pm 7.5^{s,d}$	$698 \pm 24^{s,d}$	$689 \pm 7.5^{s,d}$	$741 \pm 30^{s,d}$
	PO Peak GRF (N)	$709 \pm 8.7^{s,d}$	$660 \pm 8.8^{s,d}$	$678 \pm 9.5^{s,d}$	$700 \pm 23^{s,d}$
	Impulse ( $\text{N} \cdot \text{s}$ )	$623 \pm 6.1^s$	$496 \pm 2.5^{s,d}$	$618 \pm 11.4^s$	$496 \pm 17^{s,d}$
	Toe Clearance (cm)	$4.65 \pm 0.3^{s,d}$	$10.2 \pm 0.7^{s,d}$	$4.10 \pm 0.7^{s,d}$	$8.16 \pm 0.7^{s,d}$
S2, $0.6 \text{ m} \cdot \text{s}^{-1}$	IL Peak GRF (N)	$458 \pm 29^d$	$465 \pm 35^d$	$524 \pm 22^d$	$513 \pm 14^d$
	PO Peak GRF (N)	$497 \pm 33^s$	$437 \pm 24^{s,d}$	$528 \pm 23$	$522 \pm 23^d$
	Impulse ( $\text{N} \cdot \text{s}$ )	$360 \pm 25^s$	$268 \pm 12^s$	$367 \pm 17^s$	$317 \pm 50^{s,d}$
	Toe Clearance (cm)	$3.42 \pm 0.4^s$	$7.31 \pm 3.1^s$	$3.51 \pm 0.9^s$	$9.60 \pm 1.3^s$

s: statistically different between sides, d: statistically different between devices, s, d: statistically different between sides and devices.

and had rated his own device highly in all categories in Table 6. The subject noted that the motion of the LAP was very smooth for walking and provided good mobility, but was not confident enough in the motion yet for it to be easier to use. He also stated that it felt heavier to move than his habitual leg by the end of the walking trial. S2 habitually wore a passive 4-bar linkage knee that she rated poorly in all categories due to having issues with the knee not locking and falling often as a result of knee buckling. She was much more encouraging of the proposed LAP and stated that it helped her to not fall because it had no knee and was more stable, but also felt mobile enough to walk faster than normal. She felt more comfortable and confident when walking with the LAP than her own prosthesis.

**V. DISCUSSION AND FUTURE WORK**

**A. ELECTROMECHANICAL DESIGN EVALUATION**

The design of the length-actuated prosthesis had major improvements compared to the initial LAP device [23] and performed comparable to prostheses in other research. The physical design of the prosthesis was more compact than the initial prototype by deploying onboard sensors and actuators. When comparing overall weight of the “knee” component at 2.5 kg, the LAP was about equal to some research prototypes [9], [35], and less than several others [36], [46].

**TABLE 6.** Qualitative feedback from S1 and S2 with their HK and the LAP.

	S1		S2	
	HK	LAP	HK	LAP
Stability	10	10	1	10
Mobility	10	9	1	10
Safety	10	10	1	10
Confidence	10	4	1	9
Ease of Use	9	3	2	10
Comfort	10	2	1	10

Scale: 1 (least satisfactory) - 10 (most satisfactory).

Minimizing prosthesis weight is important because increased weight has been linked to increases in metabolic costs and decreases in gait speed, although more recent studies suggest the location of the added mass is more important and that preferences of the user are currently unclear [47], [48], [49].

The control design of the prosthesis was adaptable, which addressed main concerns from the participants’ feedback on the initial prototype [23]. The timing of the prosthesis’ motion was proven to be adaptive within one gait cycle, with negligible differences between the detected sensor cycle (input) and the time for the motion of the leg to complete

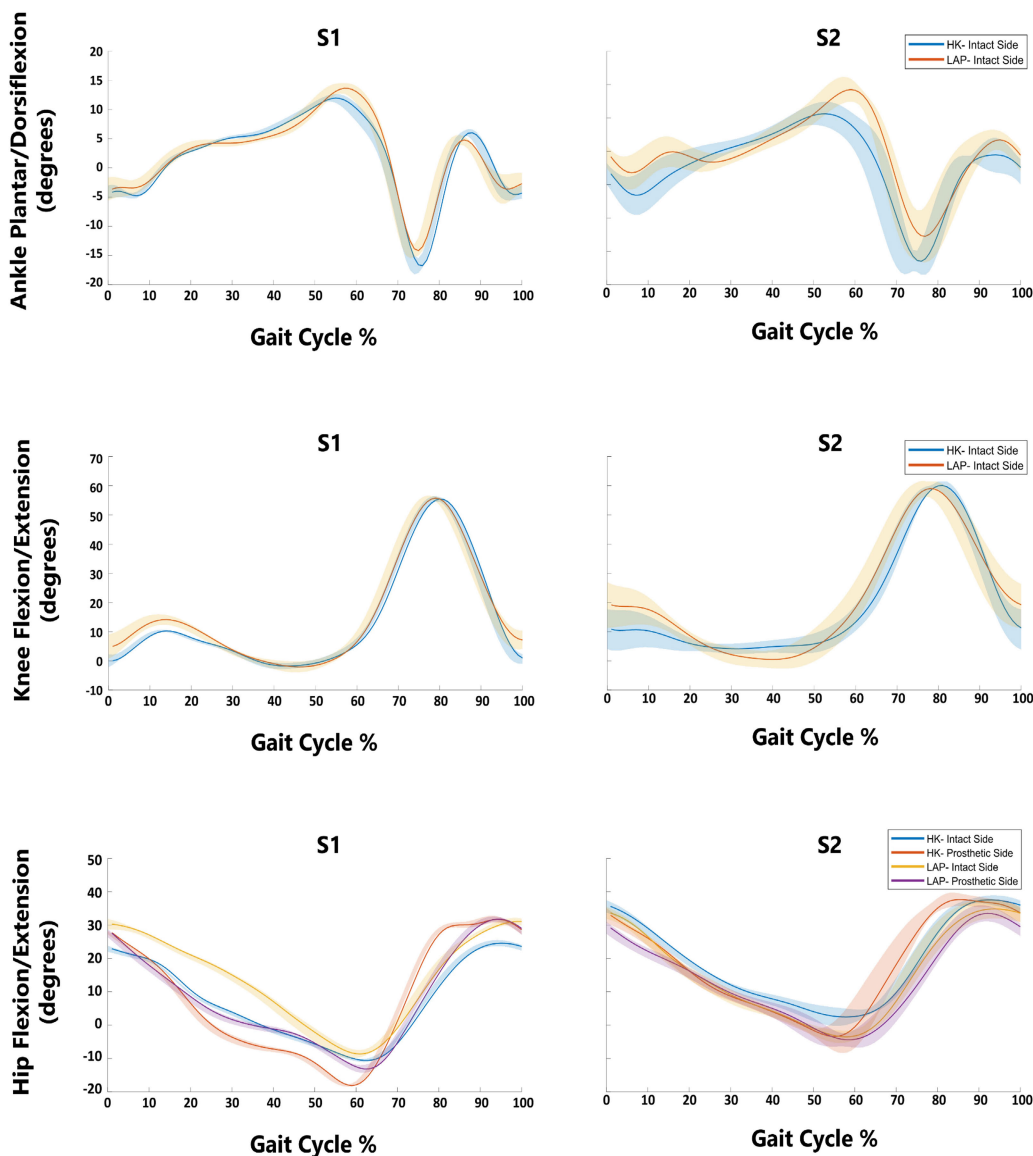


**FIGURE 11.** Mean  $\pm 1$  standard deviation of sagittal joint (ankle, knee, hip) kinematics for S1 and S2 walking at  $0.6 \text{ m} \cdot \text{s}^{-1}$  with both HK and the LAP.

(output). The actuation profile was able to match up to critical gait events within a successful threshold.

**B. BIOMECHANICAL EFFECTS ON PERSONS WITH AMPUTATION**

For testing on persons with amputation, the study focused on metrics directly affected by the LAP design (*i.e.*, toe clearance as a result of leg shortening and ground reaction forces as a result of leg lengthening). Both persons with amputation consistently exhibited higher toe clearance on their prosthetic side vs. their intact side, regardless of the device being used. While it is promising that there is sufficient toe clearance provided by the devices for swing, it is important to look into how else the user may be accomplishing toe clearance with possible altered gait biomechanics. Some may ease

toe clearance with compensations of their prosthetic side, including increased hip circumduction and hip hiking during swing [50], [51]. On the intact side, common compensations include vaulting [52], and increased hip extensor moment during stance [20], [53], [54] to aid in prosthetic side push off and to provide extra stability and height for eased toe clearance. This may be explained by the difference in ankle flexion magnitude between devices on the intact side or the early onset prosthetic side hip flexion when using the habitual prosthesis to prepare for toe clearance, but there is a need for future analyses on user’s compensatory mechanisms with the LAP.

The GRF symmetry was participant specific. The goal of leg lengthening in late stance was to induce an increased GRF for propulsion of the prosthetic limb. This was seen in the

increased push off GRFs, primarily in S1, as well as increased initial contact forces. S2 had similar but asymmetric GRFs between devices and sides. Both subjects had higher impulses and steeper GRFs on their intact side using both devices. This agrees with a study on both the C-Leg and 3R80 passive knee that there exist no prominent differences between GRFs of devices, but that critical differences exist between GRFs of the prosthetic and intact sides [55]. The intact limb had a steeper increase in GRF than the prosthetic side, and also higher overall impulses. This shows that our device has the ability to exert a GRF in late stance for push-off, but may lack the ability to provide a smooth transition to loading of the intact limb due to the steep initial loading. While the increase in push-off GRF may help reduce forward propulsion compensations, the greater initial GRF may be related to further safety concerns and is cause for further investigation/improvement.

S1 was a K3 ambulator who had been using a prosthesis for 47 years. He praised the LAP for its stability and mobility, but due to the lack of full confidence in it, he rated his own device higher. S1 also had successful GRFs that were induced for push-off by the LAP. S2 was a K2 ambulator who had been using a prosthesis for 2 years. She had major knee buckling and falling issues with her habitual device and struggled to gain confidence with it. She rated her own device poorly on stability, confidence, and ease of use and was favorable of the LAP because trusted that there would not be any knee buckling. S2 felt more comfortable and mobile with the LAP; she had much more positive feedback when comparing the device to her habitual device and an easier time adapting to the device than S1.

### C. LIMITATIONS AND FUTURE WORK

As a preliminary study, there are several limitations that can affect the interpretation of the significance as well as guide future research efforts. Firstly, the sample size is more representative of a case study analysis and thus may not give a holistic comparison between devices. For the future, the goal continues to be the recruitment of additional persons with transfemoral amputation to conduct more extensive testings for a better understanding of the device. In addition, although this study's initial primary metrics from persons with amputation are promising, it is important to perform additional biomechanical analyses on user performance with the device. Metrics could include kinematics and kinetics that provide insight to swing mobility and stance stability, which are not directly induced by the device's actuation profile (like toe clearance and push off), but are clinically important. These biomechanical metrics may also be underlying causes to the results we have presented of toe clearance and ground reaction force that are currently attributed to device performance. Even though toe clearance seems sufficient with the prosthetic devices, it would be important to investigate how gait compensations are aiding in toe clearance, as this may give insight to confidence in mobility while using the device. Additionally,

future work in classifying biomechanical effort of ambulating with the LAP (compared to a habitual prosthesis) should be explored with measures of trunk/lower limb muscle activation and overall energy consumption measures.

Current design limitations include a tethered power source and external control boxes. Although the power source and control boxes are mobile in the current design, we intend for these to be on-board the device in future iterations. With on-board controls and power, future testing and analysis would be possible for locomotion activities outside the lab. In response to the confidence/ease of use feedback from S1, future work for design includes integrating additional sensors and reducing the response time of the prosthesis for more instantaneous movement during gait phase transitions so that it instills more confidence in the user. This can be achieved by fine-tuning the placements of FSRs and the associated thresholds, as well as the incorporation of additional sensors such as inertial measurement units to categorize user intent and classify locomotor tasks. In addition, with a straight leg, the torque needed for forward progression of the entire limb is most likely higher than that of a shorter limb (with the length below the knee trailing behind). In response to the concern of the weight of the device, we will consider other lighter brushless DC motors and moving components to the proximal end of the body for design iterations.

### VI. CONCLUSION

In this paper, we proposed the design and preliminary evaluation of a novel powered length-actuated prosthesis. The prosthesis presented in this study was iterated based on previous prototypes by successfully implementing an appropriate leg length actuation profile (*i.e.*, sufficient shortening for toe clearance and lengthening for forward propulsion), a control scheme with an adjustable actuation cycle based on gait cadence, and a more compact mechanical system design less than anatomical weight requirements. Experiments with two persons with above-knee amputation demonstrated that the proposed prosthesis along with the length actuation profile are capable of producing stable and comfortable gait. Future work should focus on sensor upgrades, minimizing device weight, and continued testing on persons with amputation to better understand resulting biomechanics and perceptions.

### REFERENCES

- [1] K. Ziegler-Graham, E. J. MacKenzie, P. L. Ephraim, T. G. Trivison, and R. Brookmeyer, "Estimating the prevalence of limb loss in the united states: 2005 to 2050," *Arch. Phys. Med. Rehabil.*, vol. 89, no. 3, pp. 422–429, Mar. 2008.
- [2] J. M. Donelan, R. Kram, and A. D. Kuo, "Mechanical work for step-to-step transitions is a major determinant of the metabolic cost of human walking," *J. Experim. Biol.*, vol. 205, no. 23, pp. 3717–3727, Dec. 2002.
- [3] G. I. Papagiannis, A. I. Triantafyllou, I. M. Roumpelakis, F. Zampeli, P. G. Eleni, P. Koulouvaris, E. C. Papadopoulos, P. J. Papagelopoulos, and G. C. Babis, "Methodology of surface electromyography in gait analysis: Review of the literature," *J. Med. Eng. Technol.*, vol. 43, no. 1, pp. 59–65, Jan. 2019.
- [4] M. A. Price, P. Beckerle, and F. C. Sup, "Design optimization in lower limb prostheses: A review," *IEEE Trans. Neural Syst. Rehabil. Eng.*, vol. 27, no. 8, pp. 1574–1588, Aug. 2019.

- [5] B. Dupes, *Prosthetic Knee Systems*. Washington, DC, USA: Amputee Coalition of America, 2005, pp. 49–50.
- [6] J. L. Johansson, D. M. Sherrill, P. O. Riley, P. Bonato, and H. Herr, “A clinical comparison of variable-damping and mechanically passive prosthetic knee devices,” *Amer. J. Phys. Med. Rehabil.*, vol. 84, no. 8, pp. 563–575, 2005.
- [7] K. Bhakta, J. Camargo, W. Compton, K. Herrin, and A. Young, “Evaluation of continuous walking speed determination algorithms and embedded sensors for a powered knee & ankle prosthesis,” *IEEE Robot. Autom. Lett.*, vol. 6, no. 3, pp. 4820–4826, Jul. 2021.
- [8] A. F. Azocar, L. M. Mooney, L. J. Hargrove, and E. J. Rouse, “Design and characterization of an open-source robotic leg prosthesis,” in *Proc. 7th IEEE Int. Conf. Biomed. Robot. Biomechatronics (Biorob)*, Aug. 2018, pp. 111–118.
- [9] T. Lenzi, M. Cempini, L. Hargrove, and T. Kuiken, “Design, development, and testing of a lightweight hybrid robotic knee prosthesis,” *Int. J. Robot. Res.*, vol. 37, no. 8, pp. 953–976, Jul. 2018.
- [10] T. Elery, S. Rezaadeh, C. Nesler, and R. D. Gregg, “Design and validation of a powered Knee-Ankle prosthesis with high-torque, low-impedance actuators,” *IEEE Trans. Robot.*, vol. 36, no. 6, pp. 1649–1668, Dec. 2020.
- [11] A. Alili, V. Nalam, M. Li, M. Liu, J. Feng, J. Si, and H. Huang, “A novel framework to facilitate user preferred tuning for a robotic knee prosthesis,” *IEEE Trans. Neural Syst. Rehabil. Eng.*, vol. 31, pp. 895–903, 2023.
- [12] N. Thatte, T. Shah, and H. Geyer, “Robust and adaptive lower limb prosthesis stance control via extended Kalman filter-based gait phase estimation,” *IEEE Robot. Autom. Lett.*, vol. 4, no. 4, pp. 3129–3136, Oct. 2019.
- [13] F. Sup, H. A. Varol, J. Mitchell, T. J. Withrow, and M. Goldfarb, “Preliminary evaluations of a self-contained anthropomorphic transfemoral prosthesis,” *IEEE/ASME Trans. Mechatronics*, vol. 14, no. 6, pp. 667–676, Dec. 2009.
- [14] E. C. Martinez-Villalpando and H. Herr, “Agonist-antagonist active knee prosthesis: A preliminary study in level-ground walking,” *J. Rehabil. Res. Develop.*, vol. 46, no. 3, pp. 361–373, Jan. 2009.
- [15] J. Geeroms, L. Flynn, R. Jimenez-Fabian, B. Vanderborcht, and D. Lefeber, “Design and energetic evaluation of a prosthetic knee joint actuator with a lockable parallel spring,” *Bioinspiration Biomimetics*, vol. 12, no. 2, Feb. 2017, Art. no. 026002.
- [16] M. Katsumura, S. Obayashi, K. Yano, A. Hamada, T. Nakao, and K. Torii, “Robotic prosthesis that maintains flexion posture,” in *Proc. 41st Annu. Int. Conf. IEEE Eng. Med. Biol. Soc. (EMBC)*, Jul. 2019, pp. 6652–6655.
- [17] Y. Geng, P. Yang, X. Xu, and L. Chen, “Design and simulation of active transfemoral prosthesis,” in *Proc. 24th Chin. Control Decis. Conf. (CCDC)*, May 2012, pp. 3724–3728.
- [18] W. C. Miller, M. Speechley, and B. Deathe, “The prevalence and risk factors of falling and fear of falling among lower extremity amputees,” *Arch. Phys. Med. Rehabil.*, vol. 82, no. 8, pp. 1031–1037, Aug. 2001.
- [19] B. Carse, H. Scott, L. Brady, and J. Colvin, “A characterisation of established unilateral transfemoral amputee gait using 3D kinematics, kinetics and oxygen consumption measures,” *Gait Posture*, vol. 75, pp. 98–104, Jan. 2020.
- [20] L. Nolan and A. Lees, “The functional demands on the intact limb during walking for active transfemoral and transtibial amputees,” *Prosthetics Orthotics Int.*, vol. 24, no. 2, pp. 117–125, 2000.
- [21] R. Seliktar, “Self energized power system for above knee prostheses,” *J. Biomechanics*, vol. 4, no. 5, pp. 431–435, Oct. 1971.
- [22] R. Seliktar and R. Kenedi, “A kneeless leg prosthesis for the elderly amputee, advanced version,” *Bull. Prosthetics Res.*, vols. 10–25, pp. 97–119, Jan. 1976.
- [23] T. E. Parr, A. R. Hippensteal, and J. D. DesJardins, “Development of a length-actuated lower limb prosthesis: Functional prototype and pilot study,” *JPO J. Prosthetics Orthotics*, vol. 35, no. 2, pp. 114–121, Apr. 2023.
- [24] D. A. Winter, *Biomechanics Motor Control Human Movement*. Hoboken, NJ, USA: Wiley, 2009.
- [25] S. Khamis and E. Carmeli, “A new concept for measuring leg length discrepancy,” *J. Orthopaedics*, vol. 14, no. 2, pp. 276–280, Jun. 2017.
- [26] R. E. Hutchison, E. M. Lucas, J. Marro, T. Gambon, K. N. Bruneau, and J. D. DesJardins, “The effects of simulated knee arthrodesis on gait kinematics and kinetics,” *Proc. Inst. Mech. Eng., H, J. Eng. Med.*, vol. 233, no. 7, pp. 723–734, Jul. 2019.
- [27] P. de Leva, “Adjustments to Zatsiorsky-Seluyanov’s segment inertia parameters,” *J. Biomechanics*, vol. 29, no. 9, pp. 1223–1230, Sep. 1996.
- [28] M. Tran, L. Gabert, M. Cempini, and T. Lenzi, “A lightweight, efficient fully powered knee prosthesis with actively variable transmission,” *IEEE Robot. Autom. Lett.*, vol. 4, no. 2, pp. 1186–1193, Apr. 2019.
- [29] E. J. Rouse, L. M. Mooney, E. C. Martinez-Villalpando, and H. M. Herr, “Clutchable series-elastic actuator: Design of a robotic knee prosthesis for minimum energy consumption,” in *Proc. IEEE 13th Int. Conf. Rehabil. Robot. (ICORR)*, Jun. 2013, pp. 1–6.
- [30] E. C. Martinez-Villalpando, L. Mooney, G. Elliott, and H. Herr, “Antagonistic active knee prosthesis. A metabolic cost of walking comparison with a variable-damping prosthetic knee,” in *Proc. Annu. Int. Conf. IEEE Eng. Med. Biol. Soc.*, Aug. 2011, pp. 8519–8522.
- [31] A. Gitter, K. Paynter, G. Walden, and T. Darm, “Influence of rotators on the kinematic adaptations in stubby prosthetic gait,” *Amer. J. Phys. Med. Rehabil.*, vol. 81, no. 4, pp. 310–314, Apr. 2002.
- [32] B. Breine, P. Malcolm, S. Galle, P. Fiers, E. C. Frederick, and D. De Clercq, “Running speed-induced changes in foot contact pattern influence impact loading rate,” *Eur. J. Sport Sci.*, vol. 19, no. 6, pp. 774–783, Jul. 2019.
- [33] S. van Drongelen, M. Wesseling, J. Holder, A. Meurer, and F. Stief, “Knee load distribution in hip osteoarthritis patients after total hip replacement,” *Frontiers Bioeng. Biotechnol.*, vol. 8, Sep. 2020, Art. no. 578030.
- [34] X. Jiang, C. Napier, B. Hannigan, J. J. Eng, and C. Menon, “Estimating vertical ground reaction force during walking using a single inertial sensor,” *Sensors*, vol. 20, no. 15, p. 4345, Aug. 2020.
- [35] F. Sup, A. Bohara, and M. Goldfarb, “Design and control of a powered transfemoral prosthesis,” *Int. J. Robot. Res.*, vol. 27, no. 2, pp. 263–273, Feb. 2008.
- [36] K. Fite, J. Mitchell, F. Sup, and M. Goldfarb, “Design and control of an electrically powered knee prosthesis,” in *Proc. IEEE 10th Int. Conf. Rehabil. Robot.*, Jun. 2007, pp. 902–905.
- [37] A. H. Shultz, J. E. Mitchell, D. Truex, B. E. Lawson, and M. Goldfarb, “Preliminary evaluation of a walking controller for a powered ankle prosthesis,” in *Proc. IEEE Int. Conf. Robot. Autom.*, May 2013, pp. 4838–4843.
- [38] H. Huang, D. L. Crouch, M. Liu, G. S. Sawicki, and D. Wang, “A cyber expert system for auto-tuning powered prosthesis impedance control parameters,” *Ann. Biomed. Eng.*, vol. 44, no. 5, pp. 1613–1624, May 2016.
- [39] J. Kent and A. Franklyn-Miller, “Biomechanical models in the study of lower limb amputee kinematics: A review,” *Prosthetics Orthotics Int.*, vol. 35, no. 2, pp. 124–139, 2011.
- [40] H. R. Batten, S. M. McPhail, A. M. Mandrusiak, P. N. Varghese, and S. S. Kuys, “Gait speed as an indicator of prosthetic walking potential following lower limb amputation,” *Prosthetics Orthotics Int.*, vol. 43, no. 2, pp. 196–203, Apr. 2019.
- [41] C. K. Perera, A. A. Gopalai, S. A. Ahmad, and D. Gouwanda, “Muscles affecting minimum toe clearance,” *Frontiers Public Health*, vol. 9, May 2021, Art. no. 612064.
- [42] J. B. Ullauri, Y. Akiyama, S. Okamoto, and Y. Yamada, “Technique to reduce the minimum toe clearance of young adults during walking to simulate the risk of tripping of the elderly,” *PLoS ONE*, vol. 14, no. 6, Jun. 2019, Art. no. e0217336.
- [43] L. Johnson, A. R. De Asha, R. Munjal, J. Kulkarni, and J. G. Buckley, “Toe clearance when walking in people with unilateral transtibial amputation: Effects of passive hydraulic ankle,” *J. Rehabil. Res. Develop.*, vol. 51, no. 3, pp. 429–438, 2014.
- [44] C. A. Rábago, J. Aldridge Whitehead, and J. M. Wilken, “Evaluation of a powered ankle-foot prosthesis during slope ascent gait,” *PLoS ONE*, vol. 11, no. 12, Dec. 2016, Art. no. e0166815.
- [45] M. Ernst, B. Altenburg, M. Bellmann, and T. Schmalz, “Standing on slopes—How current microprocessor-controlled prosthetic feet support transtibial and transfemoral amputees in an everyday task,” *J. NeuroEng. Rehabil.*, vol. 14, no. 1, pp. 1–16, Dec. 2017.
- [46] C. D. Hoover, G. D. Fulk, and K. B. Fite, “Stair ascent with a powered transfemoral prosthesis under direct myoelectric control,” *IEEE/ASME Trans. Mechatronics*, vol. 18, no. 3, pp. 1191–1200, Jun. 2013.
- [47] R. S. Gailey, M. S. Nash, T. A. Atchley, R. M. Zilmer, G. R. Moline-Little, N. Morris-Cresswell, and L. I. Siebert, “The effects of prosthesis mass on metabolic cost of ambulation in non-vascular trans-tibial amputees,” *Prosthetics Orthotics Int.*, vol. 21, no. 1, pp. 9–16, 1997.
- [48] A. J. Ikeda, E. J. Hurst, A. M. Simon, S. B. Finucane, S. Hoppe-Ludwig, and L. J. Hargrove, “The impact of added mass placement on metabolic and temporal-spatial characteristics of transfemoral prosthetic gait,” *Gait Posture*, vol. 98, pp. 240–247, Oct. 2022.

- [49] B. Meikle, C. Boulias, T. Pauley, and M. Devlin, "Does increased prosthetic weight affect gait speed and patient preference in dysvascular transfemoral amputees?" *Arch. Phys. Med. Rehabil.*, vol. 84, no. 11, pp. 1657–1661, 2003.
- [50] C. L. Lewis and D. P. Ferris, "Walking with increased ankle pushoff decreases hip muscle moments," *J. Biomechanics*, vol. 41, no. 10, pp. 2082–2089, Jul. 2008.
- [51] H. M. Herr and A. M. Grabowski, "Bionic ankle-foot prosthesis normalizes walking gait for persons with leg amputation," *Proc. Roy. Soc. B, Biol. Sci.*, vol. 279, no. 1728, pp. 457–464, Feb. 2012.
- [52] J. W. Michael and J. H. Bowker, *Atlas of Amputations and Limb Deficiencies: Surgical, Prosthetic, and Rehabilitation Principles*. Rosemont, IL, USA: American Academy of Orthopaedic Surgeons, 2004.
- [53] R. E. Seroussi, A. Gitter, J. M. Czerniecki, and K. Weaver, "Mechanical work adaptations of above-knee amputee ambulation," *Arch. Phys. Med. Rehabil.*, vol. 77, no. 11, pp. 1209–1214, Nov. 1996.
- [54] J. S. Rietman, K. Postema, and J. H. B. Geertzen, "Gait analysis in prosthetics: Opinions, ideas and conclusions," *Prosthetics Orthotics Int.*, vol. 26, no. 1, pp. 50–57, 2002.
- [55] M. Schaarschmidt, S. W. Lipfert, C. Meier-Gratz, H.-C. Scholle, and A. Seyfarth, "Functional gait asymmetry of unilateral transfemoral amputees," *Hum. Movement Sci.*, vol. 31, no. 4, pp. 907–917, Aug. 2012.

**THERESE E. PARR** received the B.S. degree in mechanical engineering from Rowan University, in 2019, and the Ph.D. degree in bioengineering from Clemson University, in 2023. Her research interests include injury biomechanics, rehabilitation, wearable sensors, and human-device integration.

**JOHN D. DESJARDINS** received the B.S. degree in mechanical engineering from Carnegie Mellon University, in 1992, the M.S. degree in mechanical engineering from the University of Pittsburgh, in 1994, and the Ph.D. degree in bioengineering from Clemson University, in 2006.

He is currently the Hambright Leadership Professor in bioengineering and the Interim Director of the Robert H. Brooks Sports Science Institute, Clemson University. He has co-authored over 300 peer-reviewed conferences or journal publications in the areas of biomechanics, biomaterials tribology, implant design, sports biomechanics, rehabilitation, engineering education, and mechanical testing.

**ALAN R. HIPPENSTEAL** received the M.D. degree from the Medical College of Pennsylvania, in 1992. He has over 30 years of experience as a Physiatrist and worked most recently under the Physical Medicine and Rehabilitation Department, Prisma Health.

**TYLER G. HARVEY** received the B.S., M.S., and Ph.D. degrees in bioengineering from Clemson University, in 2014, 2016, and 2018, respectively.

His research interests include sports biomechanics, computational modeling of living systems, and scanning probe microscopy.

**GE LV** (Member, IEEE) received the B.S. degree in automation and the M.S. degree in control theory and control engineering from Northeastern University, Shenyang, China, in 2011 and 2013, respectively, and the Ph.D. degree in electrical engineering from The University of Texas at Dallas, in 2018.

He is currently an Assistant Professor with the Department of Mechanical Engineering and Department of Bioengineering, Clemson University. Prior to joining Clemson University, in Spring 2020, he was a Postdoctoral Fellow with the Robotics Institute, Carnegie Mellon University. His research interests include the control and learning of bipedal locomotion with applications to lower-limb wearable robots. He received the Best Student Paper Award from the 2015 IEEE Conference on Decision and Control and the Faculty Early Career Development Program (CAREER) Award from the National Science Foundation, in 2024.

• • •